Molecular Cell, Volume *75*

Supplemental Information

Single-Molecule Imaging Uncovers Rules Governing Nonsense-Mediated mRNA Decay

Tim A. Hoek, Deepak Khuperkar, Rik G.H. Lindeboom, Stijn Sonneveld, Bram M.P. Verhagen, Sanne Boersma, Michiel Vermeulen, and Marvin E. Tanenbaum

Supplemental figure S1. The NMD imaging approach faithfully recapitulates key aspects of NMD - related to figure 1

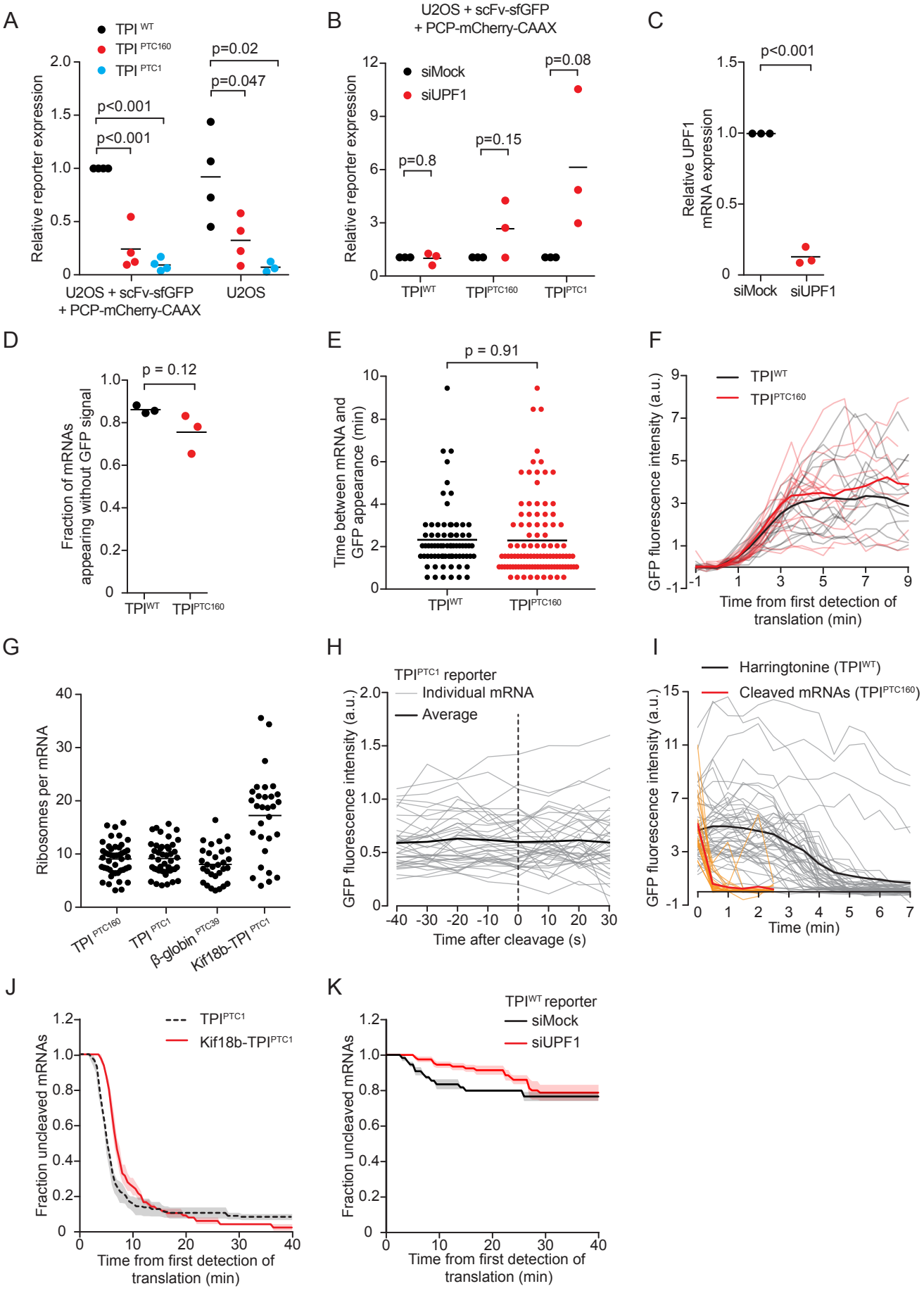

Supplemental figure S2. Additional controls to validate the NMD imaging approach related to figure 1

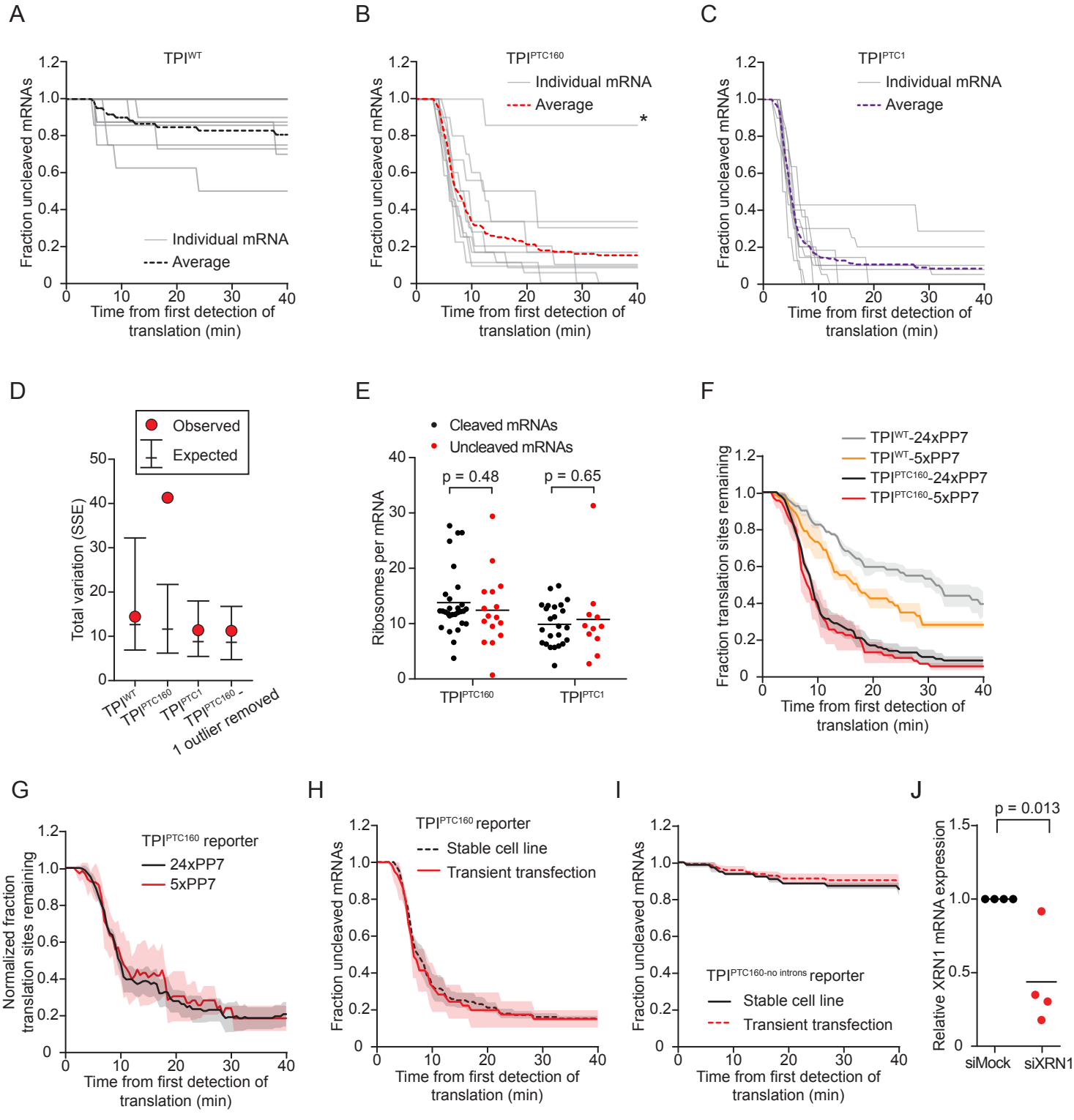

Supplemental figure S3. Multiple approaches reveal that NMD occurs with equal probability during each round of translation, related to figure 2

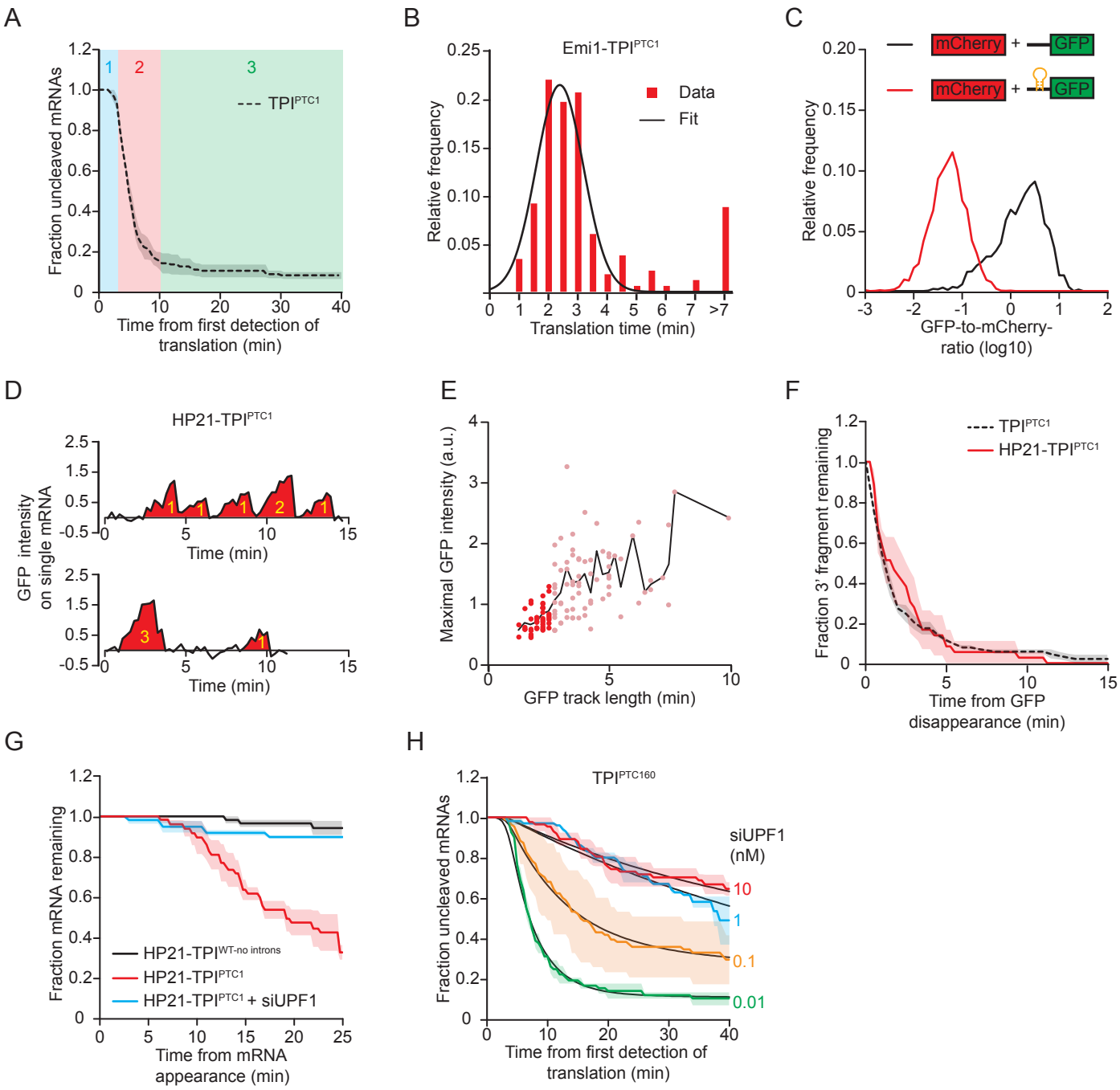

Supplemental figure S4. Kinetics of translation and NMD upon ha4E-BP1 expression - Related to figure 3

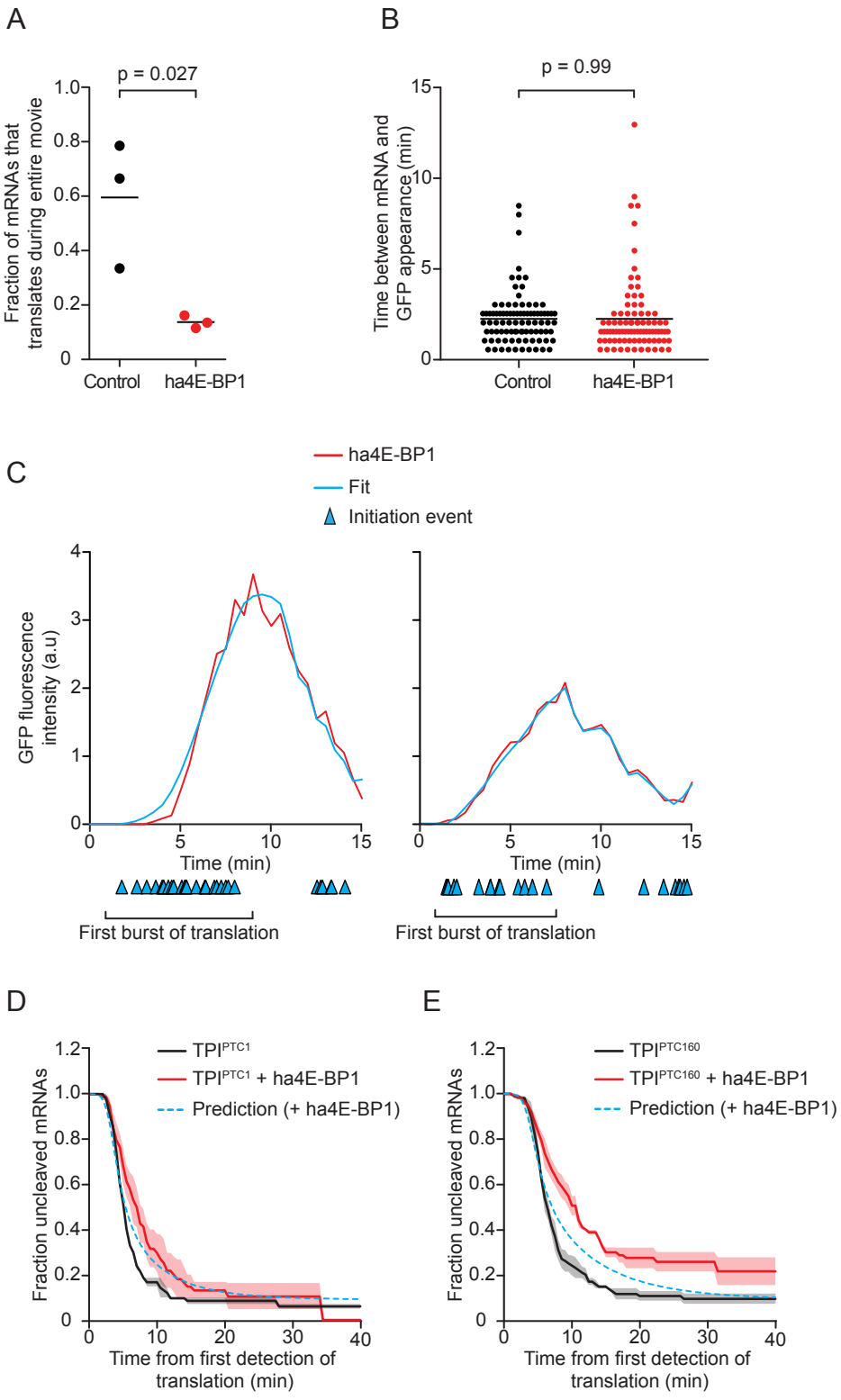

Supplemental figure S5. Splicing and decay of different NMD reporters, related to figure 4

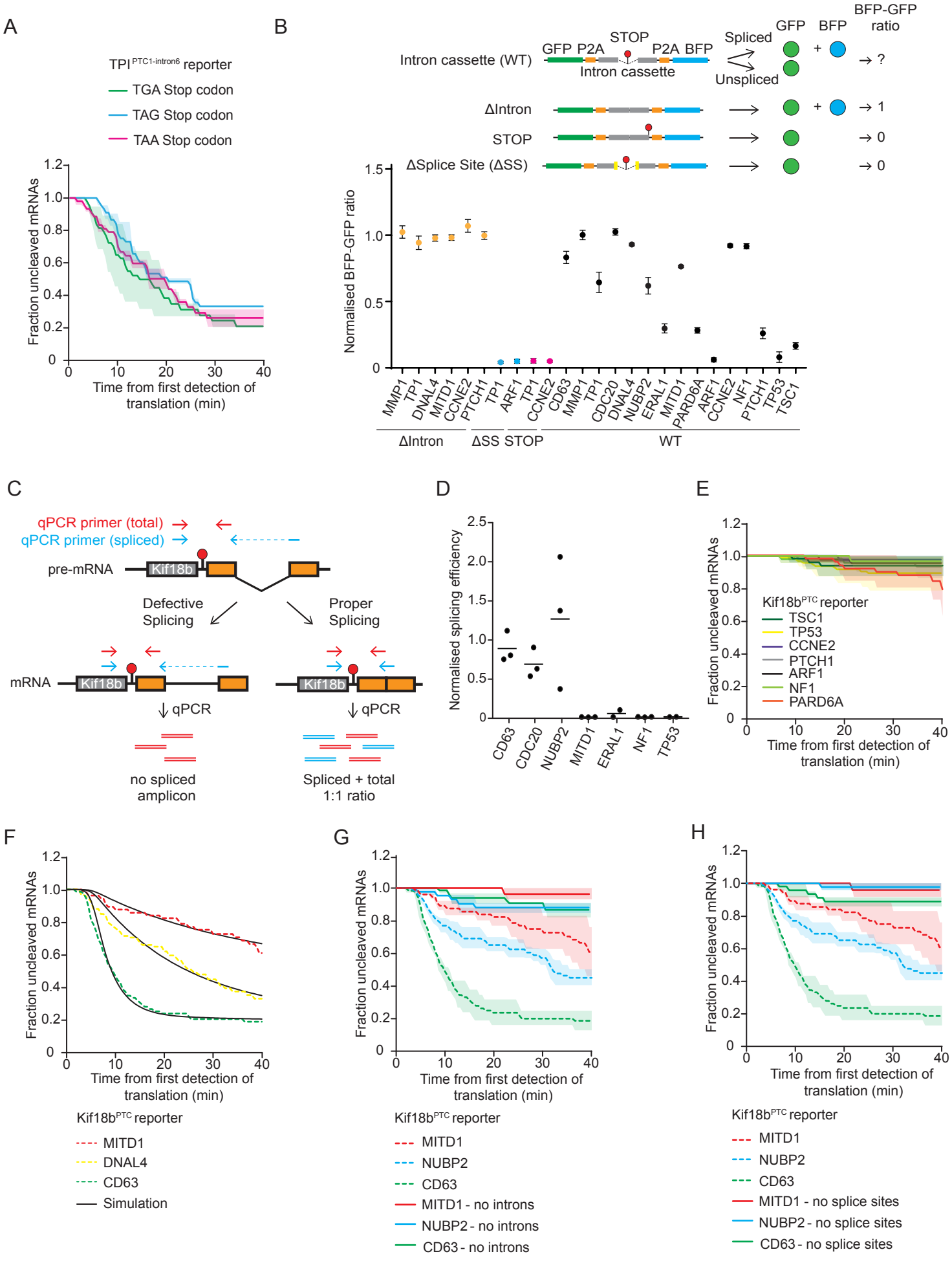

Supplemental figure S6. The PTC-to-intron distance affects the NMD decay rate, related to figure 5

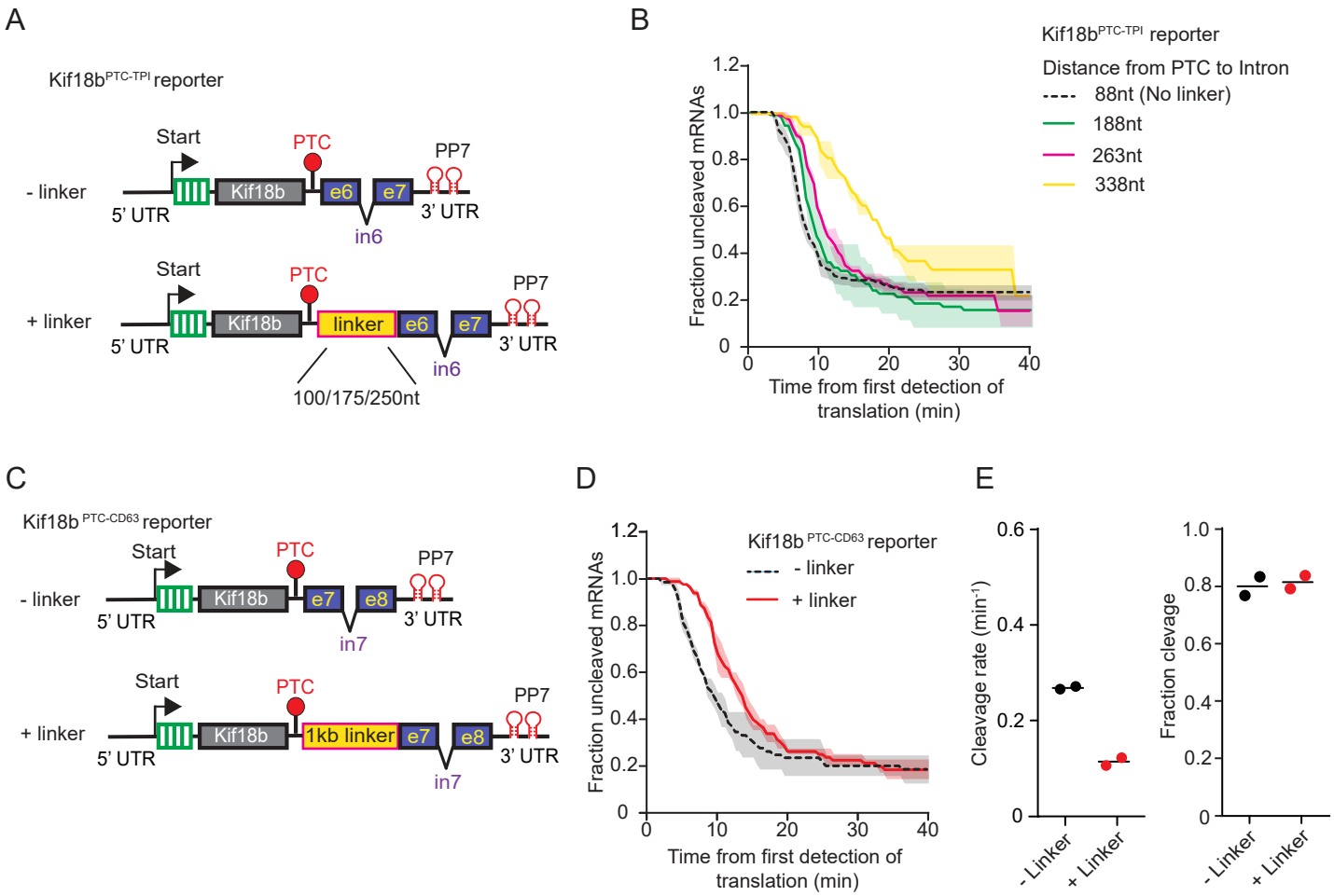

Supplemental figure S7. The number and position of introns affects the NMD decay rate, related to figure 6.

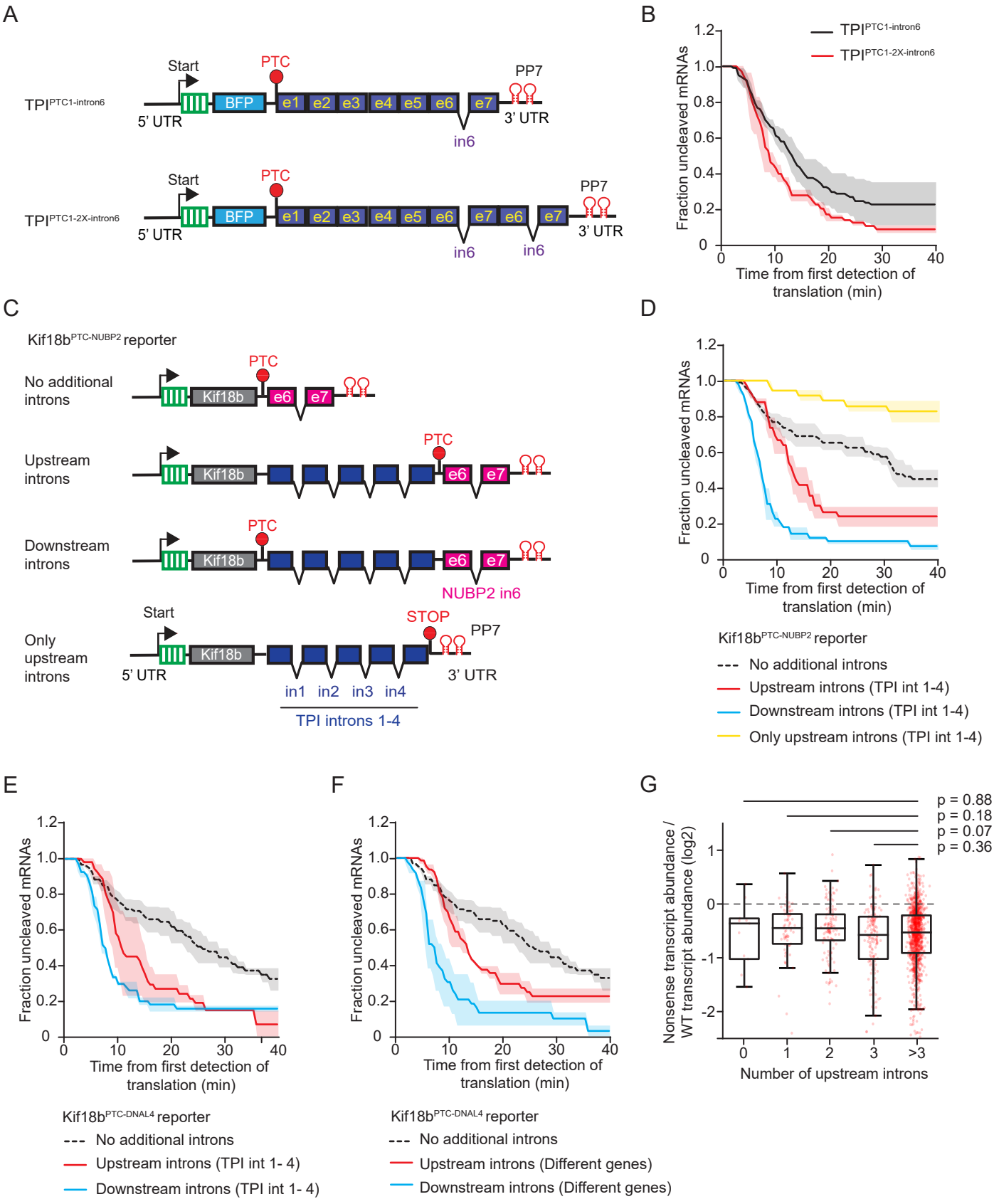

Supplemental figure legends

Supplemental figure S1 – related to figure 1. The NMD imaging approach faithfully recapitulates key aspects of NMD.

A-C) U2OS cells (A) or U2OS cells stably expressing scFv-sfGFP and PCP-mCherry-CAAX (A-C) were transfected with indicated NMD reporter plasmid and a control plasmid (A-B) and/or with indicated siRNA (B-C). mRNA abundance was assessed by qPCR and normalized to control plasmid (A-B) or GAPDH (C). Dots represent individual experiments, and the mean value is represented by a horizontal line.

(D-K) U2OS cells stably expressing scFv-sfGFP and PCP-mCherry-CAAX were transfected with indicated reporters and analyzed by time-lapse microscopy.

D) The fraction of mRNAs appearing in the field of view without an associated GFP signal was quantified for indicated reporters. Note that only mRNAs were included in this analysis that showed translation at some point in their life-time.

E) The time between appearance of the mRNA in the field of view and appearance of the first GFP signal was quantified for indicated reporters.

F) GFP fluorescence intensities were measured over time for indicated reporter mRNAs. Traces were aligned at the moment of first detection of GFP signal. Thick lines represent average intensity of all traces, thin lines represent intensity traces of individual, representative mRNAs.

G) GFP fluorescence intensities of indicated reporters were measured at the time-point immediately before cleavage for indicated reporter mRNAs. The number of ribosomes per mRNA was then determined for each mRNA (see STAR methods). Individual mRNAs (dots) and mean values (lines) are plotted.

H) Z-stacks were acquired every 10 seconds, and the GFP fluorescence intensity of individual mRNAs was measured in maximum intensity projections just prior to and immediately after mRNA cleavage (indicated by horizontal dotted line). After cleavage, the GFP spot (which no longer co-localized with the mRNA (red) spot) was tracked in 3D and its intensity was measured irrespective of it position relative to the red mRNA spot (i.e. 3' mRNA fragment). Note that the GFP signal remained constant after separation of green and red foci, indicating that all ribosomes on the mRNA molecule remained together after separation of green and red foci, consistent with mRNA cleavage rather than with sequential termination of all individual ribosomes. The thick line represents the average intensity of all traces, thin lines represent intensity traces of individual, representative mRNAs.

I) GFP fluorescence intensity of individual mRNAs was measured using an ROI centered on the location of the red mRNA spot (or 3' mRNA fragment after cleavage). For TPI^{WT} mRNAs, harringtonine was added 5 minutes after start of imaging to create a situation in which the GFP intensity associated with the mRNA

decreased due to translation termination. GFP fluorescence intensity traces of TPI^{WT} were aligned to the moment of harringtonine addition. For TPI^{PTC160} mRNAs, GFP fluorescence intensity traces were aligned to the moment of mRNA cleavage. Note that upon cleavage of TPI^{PTC160} mRNAs, the GFP fluorescence intensity drops in a single step (as the GFP spot no longer colocalizes with the mRNA), whereas the GFP signal gradually decreased over multiple time-points in harringtonine-treated cells, indicating that red-and-green foci separation is distinct from translation termination. Thick lines represents the average intensity of all traces, thin lines represent intensity traces of individual mRNAs

J, K) The time from first detection of translation until cleavage was determined for indicated reporters. Cells in (K) were treated with UPF1 siRNA 72 hr before imaging, where indicated.

All solid lines and corresponding shaded regions represent mean ± SEM. Dotted line in (J) indicates that data is replotted from an earlier figure panel Number of measurements for each experiment are listed in Table S1

Supplemental figure S2 – related to figure 1. Additional controls to validate the NMD imaging approach.

A-I) U2OS cells stably expressing scFv-sfGFP and PCP-mCherry-CAAX were transfected with indicated reporters and analyzed by time-lapse microscopy. The time from first detection of translation until cleavage was determined (A-C, H, I).

A-C) Variation in cleavage efficiency between individual cells expressing TPI^{WT} (A), TPI^{PTC160} (B), or TPI^{PTC1} (C) was examined. Individual cells in which at least 4 mRNAs were observed (thin lines) and the average of all cells (thick dotted lines) are shown. Asterisk in B) indicates a cell that shows a single outlier cell that shows inefficient cleavage.

D) Stochastic simulations were performed to determine the expected variation in cleavage kinetics among different single cells (see STAR methods). The cell-to-cell variation was quantified by calculating the summed squared error (SSE) between each individual cell in a simulation and the experimental average of all cells. This simulation was repeated 10.000 times to obtain a 95% confidence interval of the expected variation, which is indicated by error bars. Experimentally observed cell-to-cell variation (red dots) was similarly determined by calculating the SSE between individual cells and the experimental average of all cells. We observed a cell-to-cell variation that deviated substantially from the expected variation only for the experiments using the TPI^{PTC160} reporter. However, removal of a single outlier cell (indicated by asterisk in (B)) eliminated this effect (TPI^{PTC160} – outlier cell removed).

E) GFP fluorescence intensities associated with mRNAs of indicated reporters were measured 5 minutes after first detection of translation. GFP fluorescence intensities of mRNAs that would eventually be cleaved

were compared to GFP intensities of mRNAs that were not cleaved over the duration of the experiment. Individual mRNAs (dots) and mean values (lines) are plotted.

F, G) The time between appearance and disappearance of a GFP fluorescence signal was quantified for indicated reporters. Raw time-lapse microscopy data of cells expressing TPI^{PTC160} and TPI^{WT} reporters (Fig. 1D) (grey and black lines) was re-analyzed using similar criteria as the analysis of the images of cells expressing 5xPP7 reporter constructs (orange and red lines, see STAR methods).

G) Normalization of the data in (F) was performed. For each time-point, the fraction of remaining GFP foci for TPI^{PTC160} and $TPI^{PTC160\text{-}5xPP7}$ reporters was divided by the fraction of remaining GFP foci of the corresponding control reporters (TPI^{WT} and $TPI^{WT\text{-}5xPP7}$, respectively, see STAR methods).

H, I) mRNA cleavage for indicated reporters was compared in either cells transiently transfected or stably expressing the same reporter.

G) Cells were transfected with XRN1 siRNA, or were mock transfected. 72 hr after transfection, cells were harvested and XRN1 mRNA abundance was determined by qPCR. Individual experiments (dots) and mean values (lines) are plotted.

All solid lines and corresponding shaded regions represent mean ± SEM. Dotted lines indicate that data is replotted from an earlier figure panel. Number of measurements for each experiment are listed in Table S1

Supplemental figure S3 – related to figure 2. Multiple approaches reveal that NMD occurs with equal probability during each round of translation.

A-B, D-H) U2OS cells expressing scFv-sfGFP, PCP-mCherry-CAAX and indicated reporter plasmids were analyzed by time-lapse microscopy.

A) Cleavage time distribution of TPI^{PTC1} (replotted from fig. 1D) is shown. Three distinct phases in the cleavage time distribution are highlighted in different colors and numbered.

B) GFP fluorescence intensity of Emi1-TPI^{PTC1} mRNAs was analyzed, and the duration of peaks of GFP fluorescence were quantified. GFP peaks shorter than 3 frames or with high fluorescence intensity (>3-fold higher than the typical translation events) were excluded as they likely represent mRNAs translated by multiple ribosomes. The mean and variance of the elongation time were calculated from all traces of 4.5 minutes or less (as longer traces are likely to represent multiple ribosomes) by fitting the data with a Gaussian distribution (black line).

C) U2OS cells in which two plasmids, 1) mCherry and 2) either sfGFP (black line) or HP21-sfGFP (red line), were co-transfected and analyzed by FACS. The ratio of GFP and mCherry fluorescence intensities were calculated for all mCherry positive cells (averaged data of 2 independent experiments).

D) GFP intensity of HP21-TPI^{PTC1} reporter mRNAs was determined over time. Two example traces of representative mRNAs are shown, in addition to the trace shown in Fig. 2C). Red filled areas represent peaks that were called as translation events. Yellow numbers indicate the number of ribosomes that contributed to the peak.

E) Maximal GFP fluorescence intensity and duration of individual GFP peaks are plotted. Dark red dots indicate GFP peaks that likely originate from single ribosomes, while pink dots indicate peaks that may originate from more than one ribosomes based on the longer track length and/or higher GFP intensity. Black line shows the average of maximal GFP intensities for different track lengths

F) Quantification of the time between green and red foci separation and disappearance of the mRNA signal (TPI^{PTC1}), or between disappearance of the last GFP signal and disappearance of the mRNA signal (HP21-TPI^{PTC1}). Kinetics of mRNA disappearance are very similar for both conditions, suggesting that disappearance of the last GFP signal of HP21-TPI^{PTC1} followed by disappearance of the mRNA spot is an accurate readout for cleavage

G) Quantification of the time that indicated reporter mRNAs could be tracked. Cells were transfected with UPF1 siRNA 72h before imaging, where indicated. mRNA disappearance was rare in cells in which UPF1 was depleted by siRNA or in cells expressing a reporter lacking introns and a PTC, suggesting that mRNA disappearance is caused by NMD.

H) The time from first detection of translation until mRNA cleavage was determined for indicated reporters. Cells were transfected with indicated concentrations of UPF1 siRNA for 72h. Black lines indicate the best fit from stochastic simulations based on the model in which NMD occurs with equal probability during each round of translation.

All solid lines and corresponding shaded regions represent mean ± SEM. Dashed line in (F) indicates that data is replotted from an earlier figure panel. Number of measurements for each experiment are listed in Table S1

Supplemental figure S4 – related to figure 3. Kinetics of translation and NMD upon ha4E-BP1 expression

A-E) U2OS cells expressing scFv-sfGFP, PCP-mCherry-CAAX and a translation reporter (A-C) or indicated reporters (D, E) were transfected with ha4E-BP1 or mock transfected and analyzed by time-lapse microscopy.

A) The fraction of mRNAs is shown for which a GFP fluorescence signal could be detected for the entire duration of the movie. Only mRNAs on which the GFP fluorescence signal appeared at least 15 minutes

before the end of imaging were included. Dots represent individual experiments and the mean value is represented by a horizontal line.

B) The time between appearance of the mRNA in the field of view and appearance of the first GFP signal was quantified for indicated reporters.

C) Two additional example traces of representative mRNAs of cells expressing ha4E-BP1 (as in Fig 3E). Red lines indicate the experimentally observed GFP intensity over time. Blue lines indicate the best fit from simulations. Blue triangles indicate translation initiation events.

D-E) Quantification of time between first detection of translation and mRNA cleavage for indicated reporters with (red line) or without (black line) overexpression of ha4E-BP1. Dotted blue lines indicate the cleavage kinetics that are predicted upon ha4E-BP1 overexpression based on the reduced initiation rate in fig 3F (STAR methods).

All solid lines and corresponding shaded regions represent mean ± SEM. Number of measurements for each experiment are listed in Table S1

Supplemental figure S5 – related to figure 4. Splicing and decay of different NMD reporters.

A, E-H), U2OS cells expressing scFv-sfGFP, PCP-mCherry-CAAX were transfected with indicated reporter constructs and analyzed by time-lapse microscopy. Time between first detection of translation and mRNA cleavage was determined.

B) Splicing of reporters containing a single exon-intron-exon cassettes ('intron cassettes') from different genes. Schematic of splicing reporter (top). Intron cassettes were inserted between GFP and BFP. P2A ribosome skipping sites were inserted between GFP and the intron cassette, and between the intron cassette and BFP. Three types of control reporters were generated, reporters lacking an intron, reporters lacking an intron and including an in-frame stop codon immediately upstream of the BFP and reporters in which the splice sites were mutated. B, Bottom) U2OS cells were transfected with plasmids containing indicated intron cassette reporters and fluorescence intensity of BFP and GFP was measured by FACS. Spliced mRNAs produce both GFP and BFP, while unspliced mRNAs only produce GFP. BFP-to-GFP ratio was determined for each cell and the average BFP-to-GFP ratio was calculated for all cells. Average BFP-to-GFP ratio was normalized to the average BFP-to-GFP ratio of 6 reporters lacking an intron (Δintron). Dots and error bars represent mean ± SEM.

C) Schematic of the qPCR-based splicing assay. U2OS cells were transfected with Kif18b^{PTC} reporters containing indicated intron cassette, or a matched reporter from which the intron was removed. Abundance of the mRNA was assessed with a primer set that amplifies a product independently of the splicing status ('total'), and a primer set that only amplifies the spliced mRNA ('spliced'). The ratio between spliced and

total transcript abundance was determined, and normalized to the spliced/total ratio of the matched control reporters from which the intron was removed.

D) Quantification of splicing efficiencies as described in C. Dots represent individual experiments, and the mean value is represented by a horizontal line.

F) Cleavage curves of three NMD reporters with distinct decay rates. Black lines indicate the best fit from stochastic simulations based on the model in which NMD occurs with equal probability during each round of translation.

All solid lines and corresponding shaded regions represent mean ± SEM. Dashed lines in (F-H) indicate that data is replotted from an earlier figure panel. Number of measurements for each experiment are listed in Table S1

Supplemental figure S6 – related to figure 5. The PTC-to-intron distance affects the NMD decay rate.

A, C) Schematic of indicated NMD reporters.

B, D, E) U2OS cells expressing scFv-sfGFP, PCP-mCherry-CAAX and indicated reporter plasmids were analyzed by time-lapse microscopy.

B, D) The time from first detection of translation until mRNA cleavage was determined for reporters shown in (A, C)

E) The cleavage rate and fraction of mRNAs that is sensitive to NMD is presented for the data shown in (D). Each dot represents an individual experiment and lines represent the mean of 2 experiments.

All solid lines and corresponding shaded regions represent mean ± SEM. Dashed lines in (B, D) indicate that data is replotted from an earlier figure panel. Number of measurements for each experiment are listed in Table S1

Supplemental figure S7 – related to figure 6. The number and position of introns affects the NMD decay rate.

A, C) Schematic of indicated NMD reporters.

B, D-F) U2OS cells expressing scFv-sfGFP, PCP-mCherry-CAAX and indicated reporter plasmids were analyzed by time-lapse microscopy. The time from first detection of translation until cleavage was determined.

G) Genome-wide analysis of the effect of the number of upstream introns on NMD efficiency in a large cohort of cancer samples. Only PTCs with 2 or more downstream introns were included.

All solid lines and corresponding shaded regions represent mean ± SEM. In boxplots shown in (G) boxes represent the interquartile range with the central line as median, and the whiskers extend to the extreme values after removing outliers. P values are indicated as * ($p < 0.05$), ** ($p < 0.01$), *** ($p < 0.001$) by two-tailed Mann-Whitney U tests. Dashed lines in (D-F) indicate that data is replotted from an earlier figure panel. Number of measurements for each experiment are listed in Table S1